Labeling of Cerebral Amyloid β Deposits In Vivo Using Intranasal Basic Fibroblast Growth Factor and Serum Amyloid P Component in Mice

Jiong Shi, MD, PhD[1]; George Perry, PhD[2]; Marc S. Berridge, PhD[3]; Gjumrakch Aliev, MD, PhD[4]; Sandy L. Siedlak, BS[2]; Mark A. Smith, PhD[2]; Joseph C. LaManna, PhD[1]; and Robert P. Friedland, MD[1]

[1]Department of Neurology, Case Western Reserve University, University Hospitals of Cleveland, Cleveland, Ohio; [2]Department of Pathology, Case Western Reserve University, University Hospitals of Cleveland, Cleveland, Ohio; [3]Department of Radiology, Case Western Reserve University, University Hospitals of Cleveland, Cleveland, Ohio; and [4]Department of Anatomy, Case Western Reserve University, University Hospitals of Cleveland, Cleveland, Ohio

There is currently no method for noninvasive imaging of amyloid β (Aβ) deposition in Alzheimer's disease (AD). Because Aβ plaques are characteristic of AD and Aβ deposits contain abundant heparan sulfate proteoglycans that can bind basic fibroblast growth factor (bFGF) and serum amyloid P component (SAP), we investigated a novel route of ligand delivery to the brain to assess Aβ deposition in a transgenic (Tg) mouse model overexpressing Aβ-protein precursor. **Methods:** The biodistribution of bFGF injected intranasally was studied using ^{125}I-bFGF in Tg and wild-type control mice and by unlabeled bFGF and SAP immunocytochemistry with light and electron microscopy. **Results:** Three- to 5-fold higher amounts of ^{125}I-bFGF were found in the brain of Tg mice than that of wild-type mice ($P < 0.05$). bFGF or SAP given intranasally labeled cerebral Aβ plaques in the cortex and microvessels of Tg mice but not in wild-type mice. Weak bFGF staining and no SAP staining were detected in Tg mice without intranasal injection of the ligands. bFGF and SAP stained neurons around the rim of Aβ deposits and throughout the cortex in Tg mice. There was only weak staining of neurons in Tg mice without intranasal injection of bFGF and no staining of SAP in Tg mice without intranasal injection of SAP. No bFGF or SAP staining was evident in wild-type control mice. **Conclusion:** We report a novel noninvasive method for labeling Aβ plaques. This method may be modified for human studies using intranasal injection of radiolabeled ligands and imaging with SPECT or PET.

Key Words: Alzheimer's disease; cognitive disorders; dementia; amyloid β protein

J Nucl Med 2002; 43:1044–1051

Alzheimer's disease (AD), a progressive neurodegenerative disease, is the leading cause of dementia in North America and Europe. Dementia is an acquired impairment in mental abilities involving deficits in memory, language, visuospatial skills, judgment, personality, and cognition. Currently, diagnosis of AD is based on clinical symptoms and signs and the exclusion of other causes of cognitive impairment. Because of delay in recognition of AD, it is not unusual for patients to seek medical care only after the disease has become well established. Patients with AD have deposits of the amyloid β (Aβ) protein in the association cortex and limbic system. The Aβ protein is a 40- to 42-amino acid polypeptide that is deposited in brain and brain vessels as insoluble protease-resistant fibrils with a β-pleated sheet structure. It is believed that the Aβ protein is toxic to neurons and nerve terminals. Because Aβ deposition is one of the earliest and most characteristic pathologic features of AD and progression of AD is thought to be the result of an abnormal production of Aβ and of its progressive accumulation in neuritic plaques, it is important to develop a ligand to use for the noninvasive assessment of Aβ deposition in the living human brain. Such a ligand would aid in the diagnostic evaluation of patients with AD and in determining the effects of potential treatments that alter Aβ aggregation and deposition (*1*,*2*). A method of Aβ imaging will also enable researchers to investigate the neuropathologic progression of AD in its early stages in subjects with familial and sporadic forms of the disease as well as those with Down syndrome.

Studies with PET and SPECT have shown decreased cerebral metabolism of glucose and oxygen and decreased regional cerebral blood flow in the temporal and parietal cortices in the disease (*1*). Although these regional metabolic alterations are found reliably in AD, even in the early stages, they do not provide a definitive diagnosis of the

Received Sep. 18, 2001; revision accepted Jan. 22, 2002.
For correspondence or reprints contact: Robert P. Friedland, MD, Case Western Reserve University, Room TG2A, School of Medicine, 10900 Euclid Ave., Cleveland, OH 44106-4962.
E-mail: rpf2@po.cwru.edu

disease. Previously we studied SPECT imaging in AD using 10H3, a monoclonal antibody targeting Aβ protein 1–28, labeled with ^{99m}Tc (*1*,*3*). Nonspecific diffuse labeling of 10H3 around the scalp and calvarial bone marrow was found without evidence of cerebral antibody uptake (*3*). Lovat et al. (*4*) have used serum amyloid P component (SAP) labeled with ^{123}I and successfully imaged amyloid deposits in peripheral tissues of subjects with systemic amyloidosis. However, the authors were unable to show cerebral amyloid deposits in AD with SAP labeled with either ^{123}I or ^{124}I using SPECT or PET (*5*). Klunk et al. (*6*) have evaluated chrysamine G, an analog of Congo red, as a candidate molecule for Aβ imaging. Although in vitro studies showed high-affinity binding of chrysamine G to Aβ protein, no success in the in vivo studies has been reported. Iron has been found in Aβ plaques (*7*), and Bartzokis et al. (*8*,*9*) quantified brain tissue iron with MRI on the basis of the field-dependent effects of ferritin on transverse relaxation time. The iron content in AD was significantly higher in the caudate and globus pallidus than that in control subjects. However, none of these methods has been developed sufficiently to provide diagnostic or in vivo information about brain amyloid burden.

We have reported high-affinity binding of basic fibroblast growth factor (bFGF) and SAP to Aβ deposits in vitro through interactions with heparan sulfate proteoglycans in AD brain sections and transgenic (Tg) Aβ-protein precursor (AβPP) mouse brain sections (*2*). SAP has been used widely to label amyloid deposits in systemic amyloidosis (*4*,*5*). However, the delivery of bFGF (16,400 Da) to the brain cannot be achieved through the circulation because of the blood–brain barrier restriction to large molecules. SAP (235,000 Da) also has a poor blood–brain barrier penetration. Thorne et al. (*10*) have reported a quantitative analysis of drug delivery to the rat brain using the olfactory route. The only rate-limiting mechanism for an agent to enter the brain through the nose is diffusion because olfactory epithelial cells have open intercellular clefts (*11*). We have focused on the complementary approach of radioligand delivery through the nasal epithelium where olfactory bulb neurons contact the external environment directly through the cribriform plate. We report our results using a novel route of nasal injection of bFGF and SAP in mice to target Aβ protein in the brain as a possible diagnostic method for amyloid imaging in AD.

MATERIALS AND METHODS

Animals

Tg(+) mice overexpressing AβPP (all male; age, 20 mo) (*12*) and non-Tg littermate controls (all male; age, 20 mo) were obtained from Parke-Davis (Ann Arbor, MI; and Pharmacia Corp., Piscataway, NJ). They were housed at the Case Western Reserve University animal facility with a 12-h light/12-h dark cycle and free access to food and water.

Biodistribution of ^{125}I-bFGF

Three groups of experimental animals were used in studying the biodistribution of ^{125}I-bFGF: (a) Tg(+) mice with intranasal injection of ^{125}I-bFGF (2.5 MBq/μg; NEN Life Science Products, Boston, MA; human, recombinant, Bolton–Hunter labeled), $n = 5$; (b) wild-type mice with intranasal injection of ^{125}I-bFGF, $n = 5$; and (c) Tg(+) mice with intravenous injection of ^{125}I-bFGF, $n = 2$.

Mice were anesthetized by sodium pentobarbital (15 mg/kg, intraparenterally) before ^{125}I-bFGF injection. For mice in the first 2 groups, 6 drops (1.5 μL each) of ^{125}I-bFGF (1,850 kBq/μL per 10 g of body weight) were injected by a tapered-end plastic tip to each nostril, 1 drop every 5 min with the mouse supine. After each intranasal injection, the mouth was covered for 30 s to maximize penetration of ^{125}I-bFGF. For mice in the third group, the tails were warmed for 10 min under a light bulb and ^{125}I-bFGF was injected in the tail vein. Three hours after the first dose of ^{125}I-bFGF, mice were killed by pentobarbital overdose (100 mg/kg), and organs were collected and placed in weighed vials for counting the radioactivity. The brain regions were dissected into olfactory bulb, frontal and parietal cortex, hippocampus, and cerebellum according to mouse brain atlas mapping. Each injected dose was weighed and the actual injected dose was determined using standards. The standards were prepared by averaging the radioactivities of 2 mixtures of 0.1 mL distilled water and 1 μL ^{125}I-bFGF. These data were used to calculate uptake in each tissue sample in terms of percentage of injected dose per gram of tissue (%ID/g). The %ID/g was then multiplied by the measured body weight of each animal (%ID/g × animal weight/100) to obtain the normalized organ uptake, which is the fractional dose uptake per fractional body weight. The normalized uptake values were then compared with that of blood to obtain the tissue-to-blood ratio as the final value for comparison among groups (using 1-way ANOVA).

Immunocytochemistry

Three groups of experimental animals were used in the immunocytochemistry: (a) Tg(+) mice with intranasal injection of human recombinant bFGF (gift of Barbara Cordell; Scios, Sunnyvale, CA) (2.2 mg/mL in phosphate-buffered solution containing 1 mmol/L dithiothreitol [DTT] and 0.1% bovine serum albumin, pH 7.0) (Tg(+) + bFGF), $n = 7$; or Tg(+) mice with intranasal injection of SAP (Calbiochem, Mountain View, CA) (2.2 mg/mL in phosphate-buffered solution containing 1 mmol/L DTT and 0.1% bovine serum albumin, pH 7.0), $n = 6$; (b) wild-type mouse with bFGF intranasally (Tg(−) + bFGF), $n = 3$; wild-type mice with SAP intranasally (Tg(−) + SAP), $n = 3$; and (c) Tg(+) mouse with vehicle solution intranasally (Tg(+) – bFGF or SAP), $n = 6$.

All animals were anesthetized intraparenterally with pentobarbital (20 mg/kg) before intranasal injection of bFGF or vehicle solution. Six drops (1.5 μL each) of bFGF (2.2 mg/mL) or SAP (13.8 mg/mL) or vehicle solution were injected intranasally to each nostril as described. Animals were killed by pentobarbital overdose (100 mg/kg) 3 h after the first dose. Brains were collected and fixed in methacarn (methanol/chloroform/acetic acid, 6:3:1) solution for 24 h before dehydration and embedding in paraffin. Sections were cut at 6 μm and mounted on glass microscope slides coated with Silane (Sigma, St. Louis, MO).

Antibodies used included 4G8, a monoclonal antibody to Aβ-recognizing residues 17–24 (*13*); rabbit antiserum to Aβ 1–42; antibodies to the AβPP (*14*) and p141–155, a polyclonal antibody

to bFGF (gift of Barbara Cordell; Scios); and polyclonal anti-SAP (Dako Corp., Carpinteria, CA). Immunolabeling was detected by applying the peroxidase–antiperoxidase procedure with 3,3′-diaminobenzidine as cosubstrate (*2,15*). We also counterstained brain sections with Congo red. Primary antibody was omitted for the negative control.

Preembedding Immunogold Cytochemistry

Experimental AβPP Tg mice ($n = 3$) and age-matched non-Tg mice ($n = 3$) were given intranasal bFGF (44 μg) or vehicle solution. Under terminal anesthesia, mice were perfused through the heart with phosphate-buffered saline containing heparin (1,000 IU/mL) followed by 4% paraformaldehyde solution for 30 min. After perfusion, brains were immediately transfixed in 4% paraformaldehyde solution overnight. After treatment with gradient solutions of sucrose, brains were sliced using a Vibratome (The Vibratome Co., St. Louis, MO) (50–80 μm) and coronal brain sections were processed for preembedding immunogold labeling with antibodies against Aβ protein 1–42 or bFGF. Brain sections were incubated in Tris buffer solution containing 3% hydrogen peroxide and 50% methanol for 1 h at room temperature and then with 10% normal goat serum (NGS) for 1–2 h at room temperature. Sections were incubated with the primary antibody (1:500) overnight at 4°C followed by washing with 1% NGS (3 times with 10- to 15-min intervals) and incubation with 10% NGS for 10–15 min at room temperature. Samples were then incubated with gold-labeled secondary antibody (goat anti-rabbit IgG coupled to 17-nm gold, diluted in water 1:5) overnight at 4°C. After checking, the sections were rinsed to remove excess gold label. The same procedures were applied for secondary labeling using antibodies against Aβ protein or bFGF. Omission of the primary antibody was used as a control. Brain slices were postfixed in 2% glutaraldehyde overnight. The samples were then exposed to several subsequent washes and postfixed with 1% osmium tetraoxide in cacodylate buffer for 1 h. Tissues were washed again with Tris, dehydrated through the gradient concentration of alcohol and propylene oxide, and embedded in low-viscosity Spurris medium (Fisher Scientific Co., Fair Lawn, NJ). Selected brain sections were sectioned on an ultramicrotome. Thin sections were counterstained with uranyl acetate and lead citrate and examined using a JEOL 1200 CX TEM microscope (JEOL USA, Inc., Peabody, MA) operating at 80 kV.

RESULTS

Biodistribution of Nasal ^{125}I-bFGF in Periphery and Brain

Three hours after nasal injection of ^{125}I-bFGF, we detected a high uptake of radioactivity in the trachea and stomach of Tg(+) and wild-type mice. We detected 3- to 5-fold higher amounts of ^{125}I-bFGF in the olfactory bulbs and frontal, parietal, and hippocampal regions of Tg(+) mice than that of wild-type mice ($P < 0.05$) (Fig. 1A), whereas no difference was found in peripheral tissue uptake of ^{125}I-bFGF between Tg(+) and wild-type mice (Fig. 1B). Intravenous injection of ^{125}I-bFGF in either Tg(+) or wild-type mice did not produce brain uptake of bFGF, and biodistribution after intravenous injection of bFGF did not differ between Tg and wild-type mice.

Light Microscopic Study of bFGF and SAP Localization in AβPP Tg Mouse Brain

Nasally injected SAP binds to amyloid plaques in the Tg mouse brain, as detected by antibody against SAP (Fig. 2B), but not in Tg mice that did not receive SAP intranasally (Fig. 2D). Adjacent serial sections show the amyloid plaques stained for AβPP. The pattern of immunolabeling was similar to that of bFGF immunostaining. However, the intensity of immunostaining was higher with SAP than with bFGF. Nasally injected bFGF bound to neurons around Aβ deposits in the frontal, parietal, and occipital regions in Tg(+) mice (Fig. 3).

Electron Microscopic Study of bFGF Localization in AβPP Tg Mouse Brain

Tg(+) mice contained amyloid plaques throughout the brain parenchyma in the form of parallel-oriented bundle structures outside neuronal cell bodies. In Tg(+) mice that received intranasal bFGF, gold particles representing bFGF immunoreactivity were seen in the core of Aβ bundles in the cortex (Fig. 4B–4D). Tg(+) mice that did not receive a bFGF injection had no bFGF immunoreactivity in amyloid plaques (Figs. 4A and 4B), perivascular areas adjacent to amyloid deposition (Figs. 4C and 4D), or cerebral cortex and microvessels (Figs. 4B and 4C). Age-matched Tg(−) mice did not show Aβ fibers or bFGF immunolocalization.

DISCUSSION

We have used a novel noninvasive method for labeling AD brain pathology. The olfactory system is the only part of the nervous system in which neurons are in direct contact with the external environment, because the olfactory mucosa is composed of neurons transversing the cribriform openings at the base of the anterior fossa. The nose–brain barrier is porous because it lacks tight junctions. Our data showed that nasally injected bFGF and SAP enter the brain and are retained in brain regions containing Aβ plaques in AβPP Tg mice but not in wild-type mice.

We reported previously that bFGF and SAP bind to Aβ plaques in the AβPP Tg mouse brain in vitro. In this study we observed consistently by electron microscopy that after intranasal injection bFGF and SAP were present in regions where Aβ plaques were also present. Intranasally injected bFGF was found in 3- to 5-fold higher amounts in the olfactory bulb and frontal, parietal, and hippocampal regions in Tg mice compared with that in wild-type mice. The high-affinity binding of bFGF and SAP to Aβ plaques through its interaction with heparan sulfate proteoglycan provides a high signal-to-noise ratio for labeling Aβ plaques. bFGF has been shown to play an important role in regulating angiogenesis, vascular remodeling, and vascular tone, as evidenced by bFGF knockout mice that present decreased vascular smooth muscle contractility (*16,17*). bFGF is elevated in AD brain, which may be a compensatory response to vascular abnormalities in AD, including decreased capillary diameter (*18*) and atrophy of the capil-

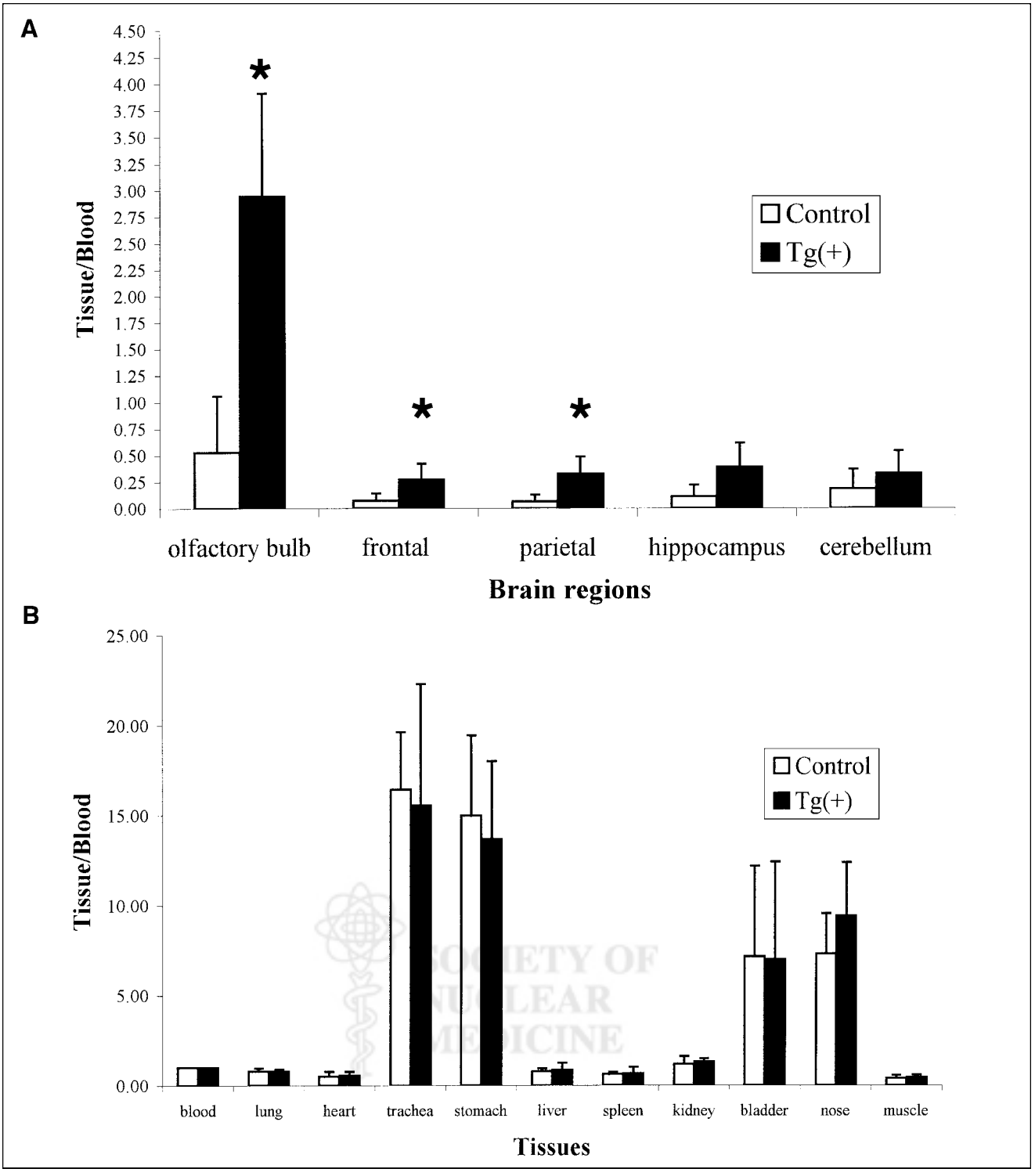

FIGURE 1. Biodistribution of ^{125}I-bFGF in 2 groups of experimental animals, Tg(+) and control, given intranasal injection of ^{125}I-bFGF (33.3 MBq/μL per 10 g of body weight). (A) Brain distribution of ^{125}I-bFGF is depicted as mean ± SD ($n = 5$ in each group). *$P < 0.05$ vs. control. (B) Whole-body distribution of ^{125}I-bFGF is depicted as mean ± SEM ($n = 5$ in each group). When SEM is not depicted, it was too small to be shown.

lary endothelium (*19*). In this study we observed that bFGF immunostaining of neurons adjacent to Aβ plaques was evident in Tg mice without bFGF input. bFGF may help these neurons directly by its trophic effects or aid them indirectly by regulating and increasing the blood supply that carries oxygen and nutrients. Alternatively, events that cause Aβ deposition may also cause bFGF and its receptor upregulation through a common pathway, such as oxidative stress.

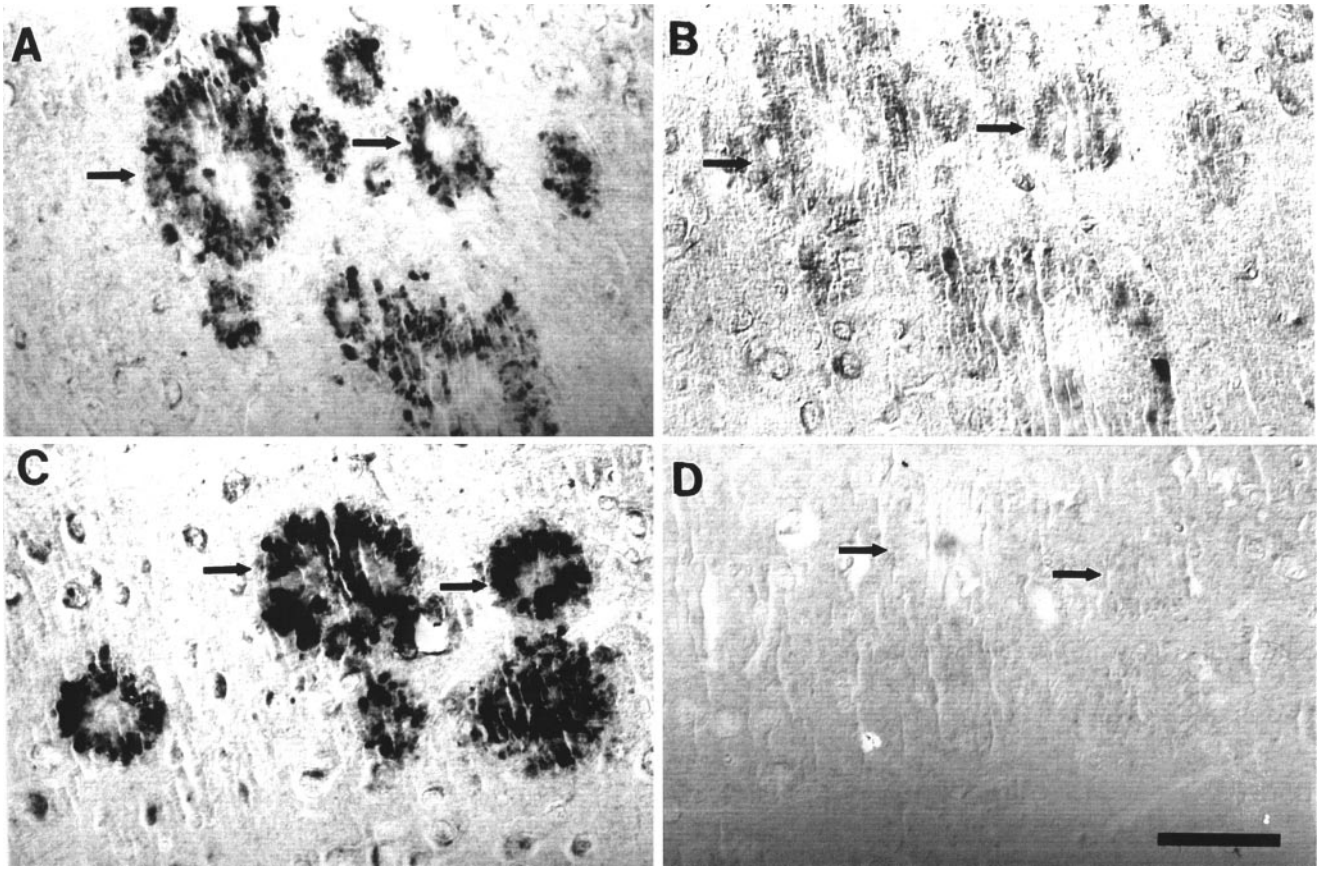

FIGURE 2. Adjacent serial sections indicate that immunostaining with antisera to AβPP shows localization of amyloid plaques (A) and that intranasally injected SAP binds to amyloid plaques in Tg mouse cortex as detected by antibody to SAP (B). (D) Brain sections from Tg mice receiving bovine serum albumin plus vehicle immunostained for SAP show no reaction in amyloid plaques, although many plaques are seen on adjacent serial sections stained for AβPP (C). Scale bar = 50 μm. Arrows mark same plaques in serial sections (A and B) and (C and D).

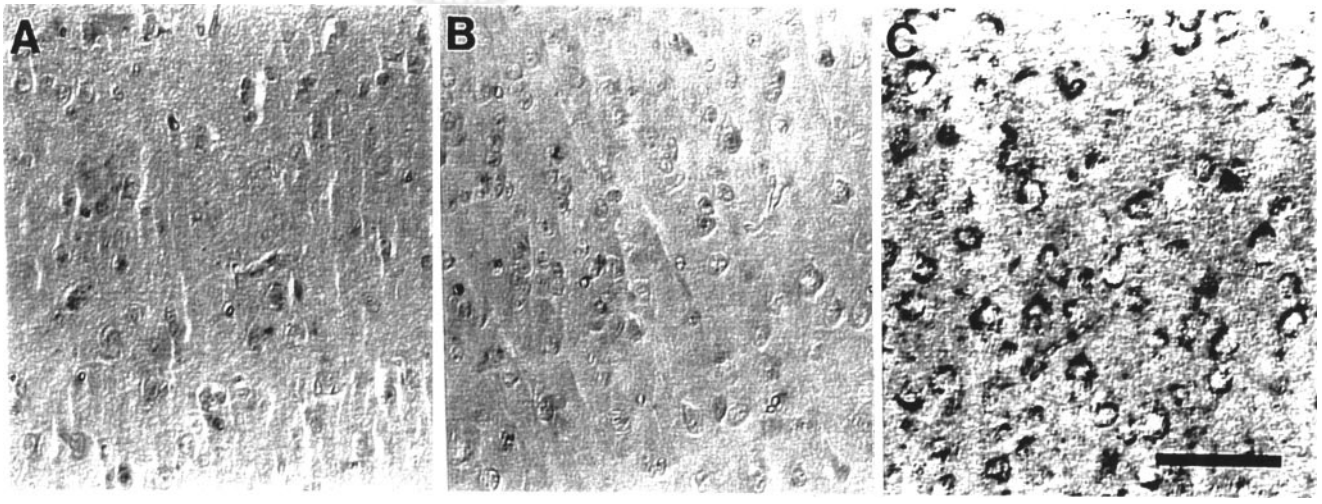

FIGURE 3. Light microscopic study of bFGF localization in AβPP Tg mouse cortex, with and without intranasal bFGF injection. bFGF is not readily detectable in neurons in Tg(−) mice after receiving bFGF intranasally (A) or in Tg(+) mice without bFGF injection (B). (C) Nasally injected bFGF bound to cytoplasm of neurons around Aβ deposits in frontal, parietal, and occipital regions in Tg(+) mice. Scale bar = 50 μm.

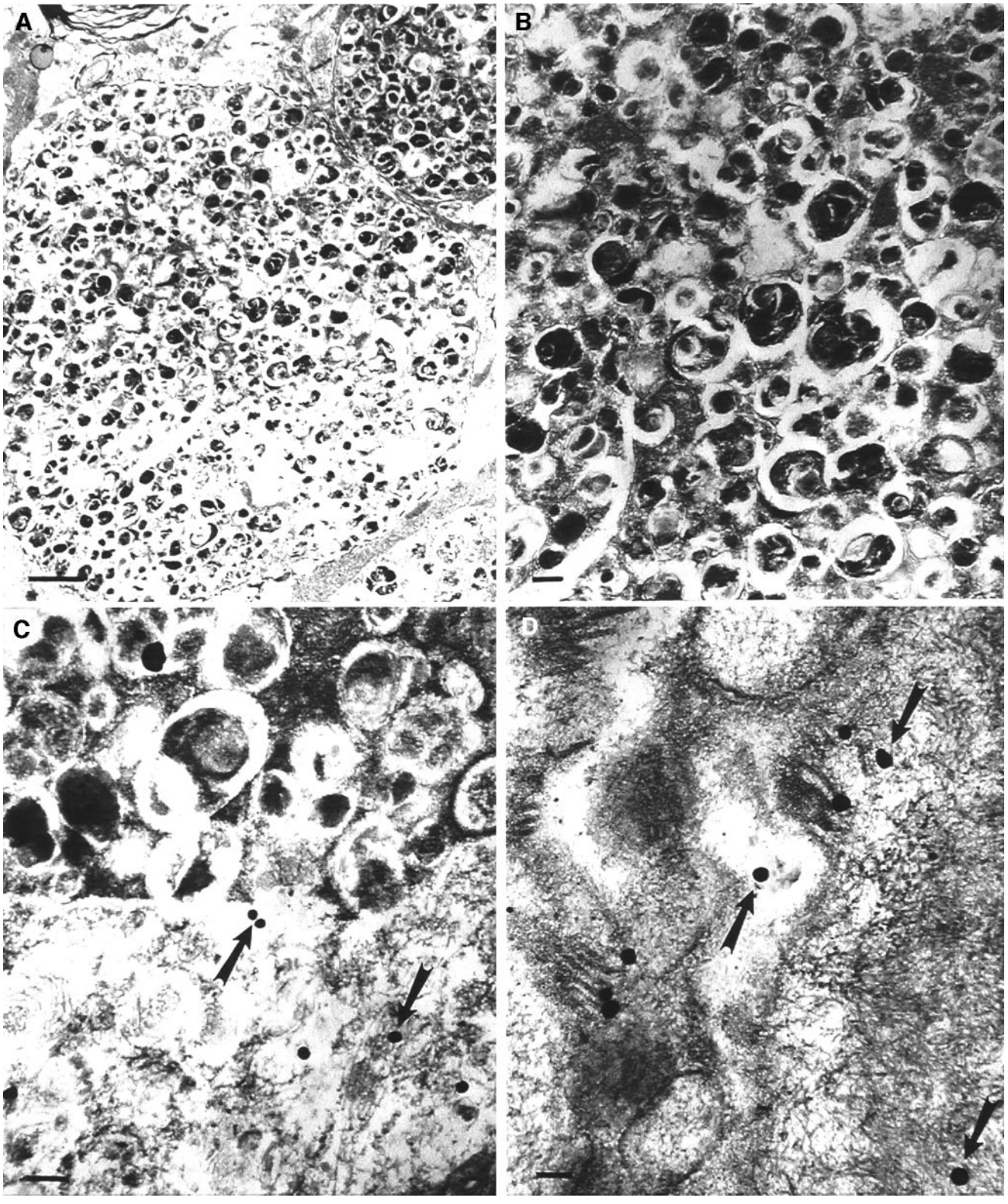

FIGURE 4. Electron microscopy immunogold staining in neuritic plaques in Tg(+) mouse cortex. (A) Tg(+) mice with intravenous injection of bFGF do not show presence of bFGF in brain (original magnification, ×8,000). (B) Same area as in A under higher magnification (×20,000). (C) Representative electron micrograph shows that peripheral margins of neuritic plaques from animals that received bFGF intranasally contain bFGF immunogold reactivity (original magnification, ×50,000). (D) bFGF is also associated with amyloid fibrils in plaque after intranasal injection (original magnification, ×50,000). Arrows indicate bFGF gold labeling. Scale bars = 10 nm.

Others have reported recent progress toward the goal of developing an amyloid imaging method useful for human studies. Skovronsky et al. (*20*) have reported a promising compound, (*trans*,*trans*)-1-bromo-2,5-bis(3-hydroxycarbonyl-4-hydroxy)styrylbenzene (BSB), that possesses the capability in binding to β-pleated structures, a major component of neurofibrillary tangles, neuritic plaques, Lewy bodies, and glial cell inclusions. BSB was shown to remain stable for at least 18 h on intrathecal or intravenous injection. The quantification of stability and binding kinetics of radiolabeled BSB is yet to be determined.

Styren et al. (*21*) have developed Congo red analogs as amyloid imaging agents in an extensive set of experiments, which have not yet included imaging. Putrescine-modified Aβ peptide has been shown to label cerebral amyloid deposits in transgenic AD mice (*22*). Barrio et al. (*23*) have used a derivative of naphthalene (2-(1-(6-[2-^{18}F-fluoroethyl)(methyl)amino]-2-naphthyl)ethylidene)malononitrile [^{18}F-FDDNP]) with PET and found entry into the brain in proportion to the blood flow, with slower clearance of the ligand from regions expected to have neurofibrillary tangles and neuritic plaques. ^{18}F-FDDNP has not yet been studied extensively in vitro, and brain uptake patterns of the molecule cannot be explained completely by binding to AD brain lesions.

PET studies of intranasally injected glucocorticoids (used to treat asthma and other respiratory conditions) have been reported in human studies of the biodistribution of drugs in the lungs and sinuses (*24*). Uptake in the sinuses on the order of 1% of the injected dose has been quantified in these PET studies. In this study we observed that most bFGF injected intranasally enters and is wasted in the trachea and lungs, which lowers the bioefficiency of bFGF uptake to the brain. This result is most likely caused by bulk aspiration of the solution during injection due to the small nasal passages of the mouse and the relatively large droplets that form. Nasal spray devices would be necessary to administer concentrated bFGF or SAP if this method were adapted for human subjects. Previous data show that nasal sprays in humans do not deposit measurable dosages into the trachea (*24*). Our method may be modified for human studies using intranasal injection of bFGF or SAP or other ligands such as Aβ or apolipoprotein E labeled with radionuclides and imaging with SPECT or PET. Fragments of the bFGF molecule may be desirable (*25*), if binding characteristics can be maintained while losing possibly hazardous growth factor properties. It would also be valuable to study the spatial and temporal distribution of bFGF or SAP and its dynamics in relation to amyloid distribution. For PET studies, radiation dosimetry and the optimal time course would also have to be determined in animal studies.

CONCLUSION

We have shown transport of bFGF and SAP to the brain through the nasal route. Nasally injected bFGF and SAP bind Aβ plaques in vivo in the AβPP Tg mouse. This relatively simple noninvasive method, using widely available neuroimaging methods, may allow for detection of AD pathology and evaluation of anti-amyloid therapy (*26*) in living patients.

ACKNOWLEDGMENTS

The authors thank Larry C. Walker, Henry LeVine, and Karen H. Ashe for their support. This research was supported in part by the Nickman family, the National Institute on Aging (grant 1UO1 AG 17173-01A2 and the Alzheimer's Disease Research Center Program, P50 AG 08012), the Joseph and Florence Mandel Foundation, The Institute for the Study of Aging (New York), and Philip Morris, USA. A preliminary account of this work was presented at the 30th Annual Meeting of the Society for Neuroscience (*27*).

REFERENCES

1. Friedland RP, Shi J, LaManna JC, et al. Prospects for noninvasive imaging of brain amyloid in Alzheimer's disease. *Ann NY Acad Sci*. 2000;903:123–128.
2. Shi J, Perry G, Aliev G, et al. Serum amyloid P is not present in amyloid beta deposits of a transgenic animal model. *NeuroReport.* 1999;10:3229–3232.
3. Friedland RP, Kalaria R, Berridge M, et al. Neuroimaging of vessel amyloid in Alzheimer's disease. *Ann NY Acad Sci.* 1997;826:242–247.
4. Lovat LB, Persey MR, Madhoo S, et al. The liver in systemic amyloidosis: insights from ^{123}I serum amyloid P component scintigraphy in 484 patients. *Gut.* 1998;42:727–734.
5. Lovat LB, O'Brien AA, Armstrong SF, et al. Scintigraphy with ^{123}I-serum amyloid P component in Alzheimer disease. *Alzheimer Dis Assoc Disord.* 1998; 12:208–210.
6. Klunk WE, Jacob RF, Mason RP. Quantifying amyloid β-peptide aggregation using the Congo red-Aβ spectrophotometric assay. *Anal Biochem.* 1999;266:66–76.
7. Smith MA, Harris PL, Sayre LM, et al. Iron accumulation in Alzheimer disease is a source of redox-generated free radicals. *Proc Natl Acad Sci USA.* 1997;94: 9866–9868.
8. Bartzokis G, Sultzer D, Mintz J, et al. In vivo evaluation of brain iron in Alzheimer's disease and normal subjects using MRI. *Biol Psychiatry.* 1994;35: 480–487.
9. Bartzokis G, Mintz J, Sultzer D, et al. In vivo MR evaluation of age-related increases in brain iron. *Am J Neuroradiol.* 1994;15:1129–1138.
10. Thorne RG, Emory CR, Ala TA, et al. Quantitative analysis of the olfactory pathway for drug delivery to the brain. *Brain Res.* 1995;692:278–282.
11. Balin BJ, Broadwell RD, Salcman M, et al. Avenues for entry of peripherally administered protein to the central nervous system in mouse, rat and squirrel monkey. *J Comp Neurol.* 1986;251:260–280.
12. Hsiao K, Chapman P, Nilsen S, et al. Correlative memory deficits, Ab elevation, and amyloid plaques in transgenic mice. *Science.* 1996;274:99–102.
13. Wisniewski HM, Wen GY, Kim KS. Comparison of four staining methods on the detection of neuritic plaques. *Acta Neuropathol (Berl).* 1989;78:22–27.
14. Cras P, Kawai M, Lowery D, et al. Senile plaque neurites in Alzheimer's disease accumulate amyloid precursor protein. *Proc Natl Acad Sci USA.* 1991;88:7552–7556.
15. Sternberger LA. The unlabeled antibody (PAP) method: introduction. *J Histochem Cytochem.* 1979;27:1657.
16. Zhou M, Sutliff RL, Paul RJ, et al. Fibroblast growth factor 2 control of vascular tone. *Nat Med.* 1998;4:201–207.
17. Bryant SR, Bjercke RJ, Erichsen DA, et al. Vascular remodeling in response to altered blood flow is mediated by fibroblast growth factor-2. *Circ Res.* 1999;84: 323–328.
18. Bell MA, Ball MJ. Morphometric comparison of hippocampal microvasculature in ageing and demented people: diameters and densities. *Acta Neuropathol (Berl).* 1981;53:299–318.
19. Perry G, Lipphardt S, Mulvihill P, et al. Amyloid precursor protein in senile plaques of Alzheimer disease [letter]. *Lancet.* 1988;355:746.

20. Skovronsky DM, Zhang B, Kung M-P, et al. In vivo detection of amyloid in a mouse model of Alzheimer's disease. *Proc Natl Acad Sci USA.* 2000;97:7609–7614.
21. Styren SD, Hamilton RL, Styren GC, et al. X-34, a fluorescent derivative of Congo red: a novel histochemical stain for Alzheimer's disease pathology. *J Histochem Cytochem.* 2000;48:1223–1232.
22. Wengenack TM, Curran GL, Poduslo JF. Targeting Alzheimer amyloid plaques in vivo. *Nat Biotechnol.* 2000;18:868–872.
23. Barrio JR, Huang S-C, Cole GM, Satyamurthy N, Petric A, Small GW. PET imaging of tangles and plaques in Alzheimer's disease [abstract]. *J Nucl Med.* 1999;40(suppl):70P–71P.
24. Berridge MS, Heald DL. In vivo characterization of inhaled pharmaceuticals using quantitative positron emission tomography. *J Clin Pharmacol.* 1999; Aug(suppl):25S–29S.
25. Xie Y, Longo FM. Neurotrophin small-molecule mimetics. *Prog Brain Res.* 2000;128:332–347.
26. Weiner HL, Lemere CA, Maron R, et al. Nasal administration of amyloid-beta peptide decreases cerebral amyloid burden in a mouse model of Alzheimer's disease. *Ann Neurol.* 2000;48:567–579.
27. Shi J, Perry G, Berridge MS, et al. Labeling of cerebral amyloid β deposits in vivo using nasally administered basic fibroblast growth factor [abstract]. *Soc Neurosci Abstr.* 2000;26:1827.